Materials Science and Engineering B 174 (2010) 242–248

Contents lists available at ScienceDirect

Materials Science and Engineering B

journal homepage: www.elsevier.com/locate/mseb

Electrodeposition and characterization of Fe doped CdSe thin films from aqueous solution

S. Thanikaikarasan[a,*], K. Sundaram[a], T. Mahalingam[a,*], S. Velumani[b], Jin-Koo Rhee[c]

[a] Department of Physics, Alagappa University, Karaikudi-630 003, India
[b] Centro de Investigación y de Estudios Avanzados del I.P.N.(CINVESTAV),Av. Instituto Politécnico,Nacional 2508,Col. San Pedro Zacatenco, 07360, México D.F
[c] Millimeter-wave Innovation Technology Research Center, Dongguk University, Seoul- 100 715, Korea

ARTICLE INFO

Article history:
Received 27 August 2009
Received in revised form 17 March 2010
Accepted 19 March 2010

Keywords:
Cadmium selenide
thin films
doping effects
optical properties
strain
dislocation density
photoelectrochemical solar cells

ABSTRACT

Thin films of Cadmium selenide (CdSe) and Ferrous (Fe) doped Cadmium selenide (CdSe:Fe) have been deposited on indium doped tin oxide coated conducting glass (ITO) substrates using potentiostatic electrodeposition technique.The mechanism of formation of CdSe and CdSe:Fe have been analyzed in the potential range between −1500 and +1500 mV versus SCE. X-ray diffraction pattern reveals that the deposited films possess hexagonal structure with preferential orientation along (002) plane. The dependency of microstructural parameters such as crystallite size, strain and dislocation density with $FeSO_4$ concentration for CdSe:Fe thin films are studied. Surface morphology and film composition shows that films with smooth surface and well defined stoichiometry is obtained at 0.01 M dopant ($FeSO_4$) concentration. Optical parameters such as band gap, refractive index and extinction coefficient for CdSe and CdSe:Fe thin films are estimated using optical absorption measurements. Photoelectrochemical solar cells are constructed using CdSe and CdSe:Fe as photocathode in 1 M each of Na_2S, S and NaOH as redox electrolyte and their power output characteristics are studied.

1. Introduction

Binary semiconductors of II-VI group attracts many researchers, because of their wide range of applications in solid state devices, such as solar cells, opto-electronic devices, solar selective coatings [1–3]. Among II-VI group semiconductors, CdSe is an important material which has been mainly utilized for photoelectrochemical solar cells and opto-electronic devices [1]. CdSe is found to be an excellent material with a direct band gap value of 1.7 eV which make them interesting for photoelectrochemical solar cells, because of their compatibility of its bandgap with the solar spectrum [4,5]. Thin films of CdSe are usually crystallized in both cubic (zinc blende) structure(JCPDS-ICDD 2003, 19-0191) with lattice constant (a = 6.077 Å) and in hexagonal (wurtzite) structure (JCPDS-ICDD 2003, 08-0459) with lattice constants (a = 4.299 Å; c = 7.010 Å). Numerous methods have been used to obtain CdSe thin films with both cubic and hexagonal structures: (i) vacuum evaporation [6], (ii) pulsed laser deposition (PLD) [7], chemical solution deposition [8]. In many of the semiconductor devices, the formation of low resistance, metal-based, ohmic contacts requires the establishment of a heavily doped region directly beneath the metal contact. If the surface layer is doped sufficiently high, the current flow across the interface proceeds principally through tunneling at the fermi level. The resistivity of polycrystalline material mainly depends upon the grain boundary or surface scattering effects [9]. The photoelectrodes based on CdSe have been observed to be susceptible to electrochemical corrosion [10]. In order to get low resistance contact, it is essential to obtain CdSe films which are doped with a suitable donor impurity concentration, the resistivity of the photoelectrode material could be reduced. Recently, much attention has been given to tailor the optical and electrical properties of these materials by using suitable dopants such as Zn, Fe and Sb [7,10,11]. The process of doping different dopants which causes the broadening of intra gap impurity bands and the formation of band tails and band gap renormalization [7]. The process of doping transition metals with CdSe find numerous applications in visible region [10]. The presence of VIII group element (such as Fe) as a dopant material with CdSe exhibit considerable effect in the number of host lattices [10]. Masumdar et al reported the growth mechanism, crystallographic, microscopic observations, optical and electrical properties of Sb doped thin films prepared using solution growth process [11]. The structural, electrical, optical and Raman spectroscopic measurements of Zn

* Corresponding author at: Department of Physics, Alagappa University, Karaikudi-630 003, India. Tel.: +91 04565 230 251/82 31 219 1847; fax: +82 31 212 9531.
E-mail addresses: S_thanikai@rediffmail.com (S. Thanikaikarasan), maha51@rediffmail.com (T. Mahalingam).

0921-5107/$ – see front matter © 2010 Elsevier B.V. All rights reserved.
doi:10.1016/j.mseb.2010.03.054

doped CdSe thin films obtained using pulsed laser deposition technique has been reported earlier by Perna et al. [7]. Among the above mentioned deposition techniques, electrodeposition provide numerous advantages over vacuum and other processes, such as low temperature growth, control of film thickness and morphology, potentially low capital cost. One obvious requirement is that the substrate must be conductive [12,16]. Pawar et al have prepared Fe doped CdSe (CdSe:Fe) thin films from non-aqueous electrolytic bath using electrodeposition technique [10]. There is no such report available for studying the effect of dopant concentration in electrodeposited CdSe:Fe thin films from aqueous electrolytic bath. Hence, an attempt is made to study the dopant concentration effect in electrodeposited CdSe:Fe thin films.

In this work, we have reported our results on the preparation and characterization of CdSe and CdSe:Fe thin films obtained from an aqueous electrolytic bath consists of $CdSO_4$, SeO_2, $FeSO_4$ and triethanolamine. The deposition mechanism has been investigated using cyclic voltammetry. Structural properties of the deposited films are analyzed using X-ray diffraction. Microstructural parameters such as crystallite size, strain and dislocation density are evaluated for CdSe:Fe thin films. Also, the morphological, compositional, optical and photoelectrochemical properties of CdSe and CdSe:Fe thin films are studied. The effect of dopant ($FeSO_4$) concentration on the above properties of the films are studied. The experimental observations are discussed in detail.

2. Experimental details

The chemicals used in this work were of Analar Grade reagents. CdSe thin films were deposited on indium doped tin oxide coated conducting glass (ITO) substrates from an aqueous electrolytic bath consists of 0.01 M $CdSO_4$, 0.01 M SeO_2. By adding adjustable amount of dilute sulphuric acid the pH of the electrolytic bath was adjusted to 2.5 ± 0.1. At lower pH value, such as below 2.5 ± 0.1 adherence of the film to the substrate was very poor. At higher pH value such as above 2.5 ± 0.1, there is precipitation of $CdSO_4$ occurs which yields films with poor quality. Hence, an optimum solution pH value of 2.5 ± 0.1 must be fixed in order to get good quality films. The electrochemical experiments were carried out using a PAR scanning potentiostat/galvanostat unit (Model 362, EG & G, Princeton Applied Research, USA) employing three electrode configuration with ITO substrate as cathode, platinum electrode as counter electrode and saturated calomel electrode (SCE) as reference electrode, respectively. Before used for deposition, ITO substrates were treated for 15 minutes with ultrasonic waves in a bath of isopropanol and then rinsed with acetone. The SCE was introduced into the solution by luggin capillary whose tip was placed as close as possible to the working electrode. Fe doped CdSe films (CdSe:Fe) was obtained by using 0.01 M $FeSO_4$ solution added in the deposition bath during the process of deposition of CdSe thin films. To obtain stoichiometric films with Fe doping, it is essential to reduce the deposition rate of Fe when compared to CdSe. This could be obtained by adding 0.005 M triethanolmine (TEA) as complexing agent with $FeSO_4$ solution. This mixture was added in an aqueous acidic bath containing $CdSO_4$ and SeO_2 in order to obtain CdSe:Fe films. The concentration of iron triethanolamine mixture was so adjusted, such that the formation of other compounds of Fe and Se were inhibited. The deposition potential was fixed as −700 mV versus SCE for CdSe and CdSe:Fe thin films using cyclic voltammetry. The films deposited at lower bath temperature such as below 80 °C were poorly crystallized, whereas the films deposited at higher bath temperature such as above 80 °C, the current densities were found to be higher. These higher current densities increase the rate of deposition which in turn causes peel of the film from the substrate. Hence, the bath temperature was fixed as 80 °C for CdSe and CdSe:Fe thin films. The optimum deposition conditions used for the preparation of CdSe and CdSe:Fe thin films were: Solution pH: 2.5 ± 0.1, Bath temperature:80 °C, Deposition potential:-700 mV versus SCE.

Cyclic voltammetric studies was taken out in a standard three compartment cell using BAS 200A electrochemical analyzer. Thickness of CdSe and CdSe:Fe films was estimated using stylus profilometer (Mitutoyo SJ 301). An X-ray diffractometer (XPERT PRO PANalytical, Netherland) with CuK_α radiation ($\lambda = 1.540$ Å) was used to identify the crystalline nature and phases of the deposited films. The surface morphology and film composition were analyzed using an energy dispersive analysis by X-rays set up attached with scanning electron microscope (JEOL JSM 840). Optical absorption spectrum of the samples was recorded using an UV-Vis-NIR spectrophotometer (HR-2000, M/S Ocean Optics, USA). Photoelectrochemical measurements of CdSe and CdSe:Fe thin films was carried out using three electrode system comprising of CdSe and CdSe:Fe thin film as photocathode, platinum electrode as counter electrode and SCE as reference electrode, respectively.

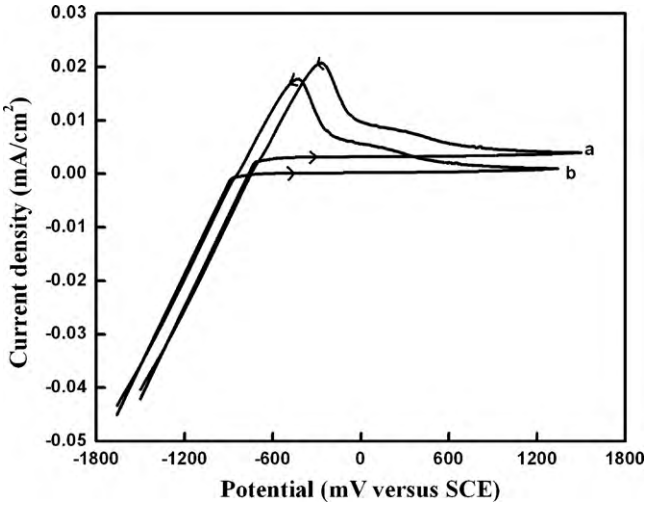

Fig. 1. Cyclic voltammogram of ITO glass electrode: (a) Electrolyte solution mixture containing 0.01 M $CdSO_4$ and 0.01 M SeO_2. (b) Electrolyte solution mixture containing 0.01 M $CdSO_4$, 0.01 M $FeSO_4$,0.01 M SeO_2 and 0.005 M TEA.

3. Results and Discussion

3.1. Cyclic voltammetric studies

Cyclic voltammetry is a powerful analytical tool for studying electrochemical reaction in solutions of $CdSO_4$, SeO_2 and $FeSO_4$. Cyclic voltammetric studies was performed in a standard three electrode cell consists of ITO substrate as cathode, platinum electrode as anode and SCE as reference electrode, respectively. The scan rate employed was 20 mV/sec. The voltammetric curves were scanned in the potential range from −1500 to +1500 mV versus SCE. Fig. 1a shows the typical cyclic voltammogram recorded for ITO glass electrode in an aqueous solution mixture containing 0.01 M $CdSO_4$ and 0.01 M SeO_2. It is observed from Fig. 1a, that the growth of CdSe starts at a potential −717 mV versus SCE. During cathodic scan, the reoxidation peak observed at −600 mV versus SCE which is responsible for superimposed peaks of compound CdSe and element Cd, since this peak is similar to pure solution of $CdSO_4$ and hence no oxidation peak of CdSe is found. A hysteresis is obtained in the potential range between −717 and −699 mV versus SCE indicates that the deposition of CdSe occurs more easily on the CdSe surface than those on ITO surface, since the working electrode is initially covered with CdSe instead of ITO. Hence, the formation of CdSe starts at a more positive deposition potential on the surface of CdSe electrode [13]. The reduction of H_2SeO_3 to Se is the rate controlling step in the deposition process, the first is the reduction of Cd^{2+} to Cd on the surface of ITO electrode which is followed by electrochemical reduction of H_2SeO_3 with element Cd according to the following Eq. (1).

$$Cd + H_2SeO_3 + 4H^+ + 4e^- \rightarrow CdSe + 3H_2O \quad (1)$$

Fig. 1b shows the cyclic voltammogram recorded for ITO glass electrode in an aqueous solution mixture containing 0.01 M $CdSO_4$, 0.01 M SeO_2, 0.01 M $FeSO_4$ and 0.005 M TEA as complexing agent. A slight shift in oxidation and reduction potential observed may be due to the addition of $FeSO_4$ and TEA in an aqueous solution mixture consists of $CdSO_4$ and SeO_2. The co-deposition of Fe along with CdSe which is confirmed from elemental compositional analysis.

3.2. Film thickness

The electrochemical growth of CdSe and CdSe:Fe thin films is controlled by two separate variables such as (i) film thickness and

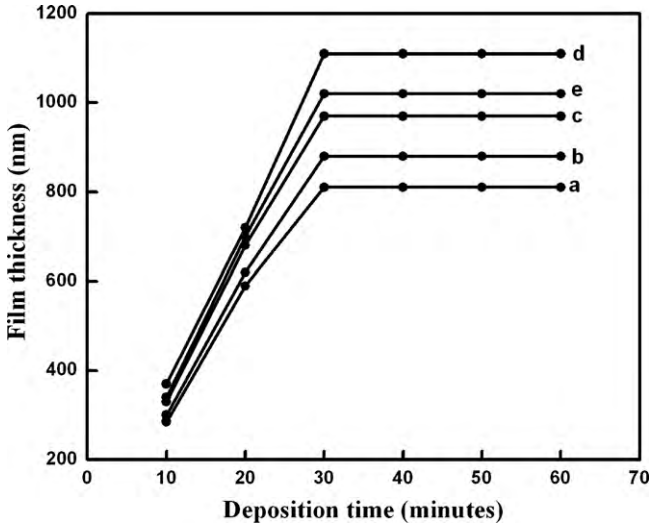

Fig. 2. Variation of film thickness with deposition time: (a) CdSe and CdSe:Fe thin films prepared at various $FeSO_4$ concentrations: (b) 0.0025 M (c) 0.005 M (d) 0.01 M (e) 0.02 M.

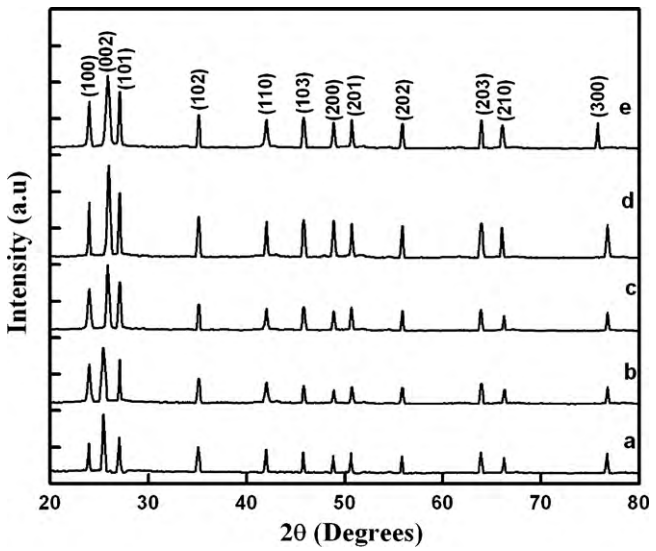

Fig. 3. X-ray diffraction patterns: (a) CdSe and CdSe:Fe thin films prepared at various $FeSO_4$ concentrations: (b) 0.0025 M (c) 0.005 M (d) 0.01 M (e) 0.02 M.

its uniformity (ii) surface morphology. The bath temperature is expected to influence the deposition rate by (i) increase of precursor solubility and decrease in value of viscosity [12]. Due to increase in solubility with bath temperature higher value of film thickness is obtained for CdSe and CdSe:Fe thin films prepared at bath temperature of 80 °C. Thickness of the deposited films is measured using stylus profilometer. The average thickness of the deposited films can be directly controlled by controlling the plating current and plating time. Fig. 2a shows the variation of film thickness with deposition time for CdSe thin film obtained at bath temperature of 80 °C. It is observed from Fig. 2a that the film thickness increases linearly with deposition time and tend to attain saturation after 30 minutes of deposition. Further increasing deposition time above 30 minutes, thickness of the film remains constant. The variation of film thickness with deposition time for CdSe:Fe thin films prepared at bath temperature of 80 °C under different $FeSO_4$ concentrations are shown in Fig. 2 (b-e). Fig. 2(b-d) indicates that thickness of the film increases linearly with deposition time and attained its maximum value for films prepared at a deposition time of 30 minutes. The maximum value of film thickness is obtained for films prepared at 0.01 M $FeSO_4$ concentration at a deposition time of 30 minutes. Further increasing the $FeSO_4$ concentration above 0.01 M, results decrease in value of film thickness which is shown in Fig. 2e. This can be explained by the following mechanism. First, the role of an Fe atom acts as a nucleation centre upto (i.e) 0.01 M doping level (the content of Cd and Fe are: 46.12% and 0.86%), enhances the growth process and therefore the film thickness (Fig. 2(b-d)). Further increasing doping concentration above 0.01 M, Fe may occupy the interstitial sites causes an impurity scattering and thereby preventing further film formation [11,14].

3.3. Structural studies

X-ray diffraction (XRD) pattern obtained for CdSe and CdSe:Fe films on ITO substrates at a bath temperature of 80 °C under various $FeSO_4$ concentrations from 0.0025 to 0.02 M are shown in Fig. 3(a-e). Fig. 3a revealed that the deposited films exhibits hexagonal structure with lattice constant value (a = 4.299 Å; c = 7.010 Å)(08-0459) [15]. The observed values of lattice constants are found to be ± 0.03 difference from standard values. The observed diffraction peaks of hexagonal CdSe are found at 2θ values of angles 23.92, 25.84, 27.01, 35.07, 41.93, 45.76, 48.80, 50.62, 55.81, 63.87, 66.20, 76.69 corresponding to the lattice planes (100), (002), (101), (102), (110), (103), (200), (201), (202), (203), (210) and (300), respectively]. All the peaks intensities identified are from CdSe and hence no additional lines corresponding to Cd and Se are present. The height of (002) plane is found to be higher than all other peaks in the diffractogram (Fig. 3(a-e)), represents that the crystallites are preferentially oriented along (002) plane. This represents that electrodeposition method is suitable for the preparation of single phase hexagonal CdSe films. The 'd' values observed in the present work are found to be in good agreement with JCPDS file for hexagonal CdSe [15]. XRD pattern of CdSe:Fe thin films on ITO substrates at various $FeSO_4$ concentrations from 0.0025 to 0.02 M is shown in Fig. 3 (b-e). It is observed from Fig. 3 (b-e) that the diffraction peaks of CdSe:Fe are found at 2θ values of angles 23.97, 25.89, 27.09, 35.13, 42.01, 45.87,48.82, 50.72, 55.87, 63.92, 66.12, 76.77 corresponding to the lattice planes(100), (002), (101), (102), (110), (103),(200),(201),((202),(203),(210) and (300) respectively. By comparing Fig. 3a and (b-e) a slight shift in diffraction line is observed. This may be due to the incorporation of small quantity of Fe in the deposition bath, therefore Fe peaks are not seen in XRD pattern. No major difference is observed in XRD pattern for CdSe and CdSe:Fe thin films. However, the sharpness of the peak increases which in turn decreases the FWHM data results increase in value of crystallinity of CdSe:Fe thin films. The effect of $FeSO_4$ concentration on the orientation of polycrystalline CdSe:Fe thin films are investigated by evaluating the texture coefficient (T_c(hkl)) of the (hkl) plane using the following Eq. (2) [16].

$$T_c(hkl) = \frac{I(hkl)/I_0(hkl)}{(1/N)\left(\sum_N I(hkl)/I_0(hkl)\right)} \quad (2)$$

where T_c(hkl) is the texture coefficient of the (hkl) plane, I is the measured intensity and I_0 is the JCPDS standard intensity, N is the number of diffraction peaks. From the above Eq. (2), it is seen that the value of texture coefficient approaches unity for a randomly distributed powder sample, while T_c(hkl) is greater than unity when the (hkl) plane is preferentially oriented [16]. Fig. 4 shows the variation of texture coefficient with respect to $FeSO_4$ concentration for CdSe:Fe thin films prepared at various $FeSO_4$ concentrations. It is observed from Fig. 4, that the lower value of texture coefficient represents that the films have poor crystallinity and the

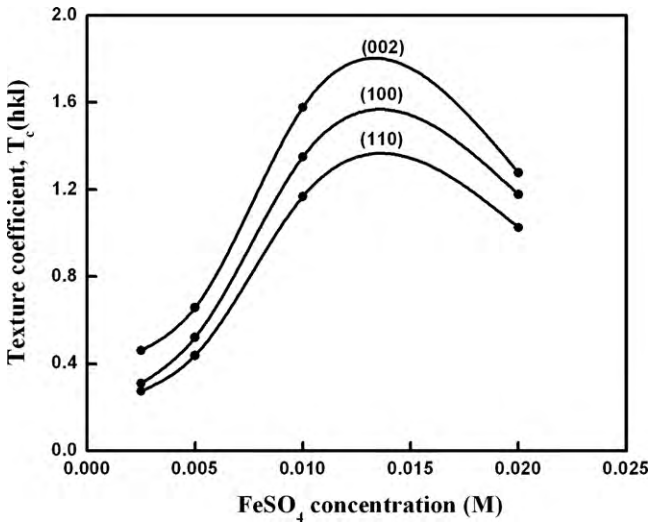

Fig. 4. Variation of texture coefficient along the (100), (110) and (002) planes for CdSe:Fe thin films prepared at various $FeSO_4$ concentrations.

crystallinity may be improved by increasing the $FeSO_4$ concentration from 0.0025 to 0.01 M. Further increasing $FeSO_4$ concentration above 0.01 M, the value of texture coefficient slightly decreases as shown in Fig. 4. Hence, CdSe:Fe films obtained at 0.01 M concentration have better crystallinity and well adherent to the substrates. The crystallite size of all the deposited films (CdSe and CdSe:Fe) can be determined from FWHM data using Debye-Scherrer's formula (Eq. (3)) [12,16]

$$D = \frac{0.9\lambda}{\beta \cos\theta_B} \tag{3}$$

where β is Full Width at Half Maximum of the peak in radian, λ is the wavelength of CuK_α target (λ = 1.540 Å), θ_B is Bragg diffraction angle at peak position in degrees. The crystallite size of all the deposited films (CdSe and CdSe:Fe) obtained in the present work are found to be in the range between 47 and 54 nm. The strain ε was calculated from the slope of β cosθ versus sinθ plot using the following Eq. (4) [12].

$$\beta = \left[\frac{\lambda}{D\cos\theta}\right] - \left[\varepsilon \tan\theta\right] \tag{4}$$

Dislocation density is defined as the length of dislocation line per unit volume of the crystal (Williamson and Smallman) [12,17]. Dislocation density is given by the following Eq. (5)

$$\delta = \frac{1}{D^2} \tag{5}$$

X-ray diffraction pattern of CdSe and CdSe:Fe films prepared under various $FeSO_4$ concentrations are recorded. Using FWHM data and Debye-Scherrer's formula, the crystallite size of the deposited films are calculated. From the slope of βcosθ versus sinθ and using Eq. (4) the strain (ε) in the film is calculated. Fig. 5a shows the variation of crystallite size and strain with $FeSO_4$ concentration for CdSe:Fe thin films prepared at various $FeSO_4$ concentrations from 0.0025 to 0.02 M. The variation of dislocation density with $FeSO_4$ concentration for CdSe:Fe thin films obtained at various $FeSO_4$ concentrations is shown in Fig. 5b. It is observed from Fig. 5a, that the crystallite size increases with $FeSO_4$ concentration and the films prepared at 0.01 M $FeSO_4$ concentration are found to have maximum value of crystallite size, thereafter the crystallite size slightly decreases. Due to the release of defects in the lattice, strain in the film gets released and attained its minimum value for films obtained at 0.01 M $FeSO_4$ concentration. A sharp increase in crystallite size and decrease in strain with $FeSO_4$ concentration is

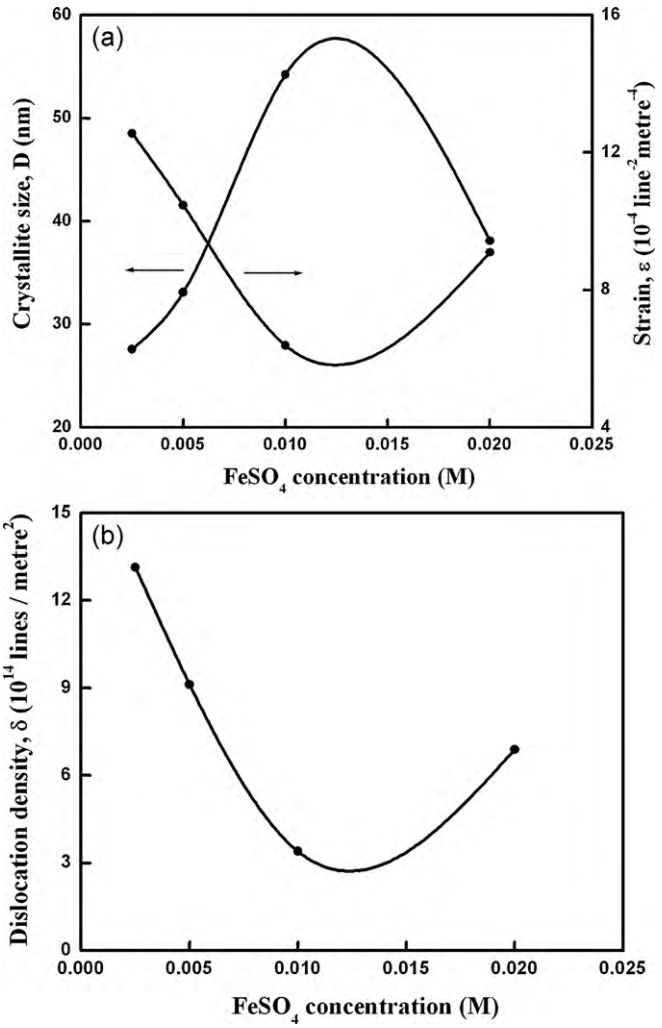

Fig. 5. (a) Variation of crystallite size and strain with $FeSO_4$ concentration for CdSe:Fe thin films prepared at various $FeSO_4$ concentrations; (b) Variation of dislocation density with $FeSO_4$ concentration for CdSe:Fe thin films prepared at various $FeSO_4$ concentrations.

indicated in Fig. 5a. Decrease in value of strain with $FeSO_4$ concentration results decrease in value of interplanar spacing thus leads to decrease in value of dislocation density which is shown in Fig. 5b. Minimum values of strain and dislocation density are obtained for films prepared at $FeSO_4$ concentration of 0.01 M. CdSe:Fe films with lower strain and dislocation density improves the stoichiometry of the films which is turn causes volumetric expansion of films. Studies on functional dependency of crystallite size, strain and dislocation density with $FeSO_4$ concentration represents that the strain and dislocation density decreases, whereas the crystallite size increases [12].

3.4. Surface morphology and film composition

The surface morphology of CdSe and CdSe:Fe thin films is analyzed using a scanning electron microscope. The surface morphology of CdSe and CdSe:Fe thin films prepared under optimized condition is shown in Fig. 6a,b. By comparing Fig. 6a and b the surface is found to be quite same for both CdSe and CdSe:Fe thin films. Fig. 6b shows that the surface is observed to be smooth and covered with uniform spherically shaped grains. The grains are distributed uniformly over the entire surface of the film. Some flaws are seen at few places in SEM picture (Fig. 6b). The addition of $FeSO_4$ in electrolytic bath results increase in value of grain size for CdSe:Fe

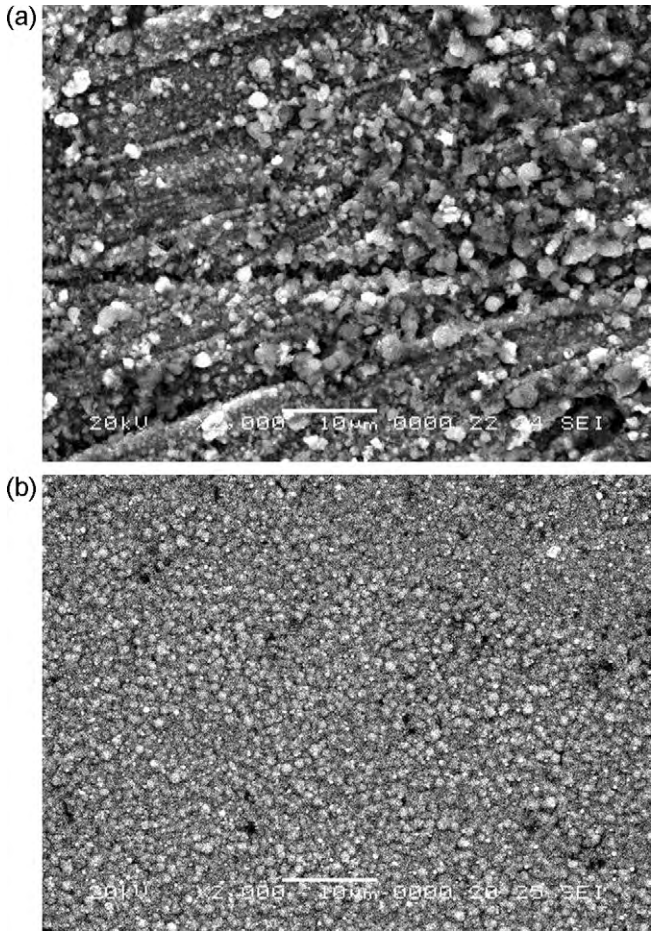

Fig. 6. (a) SEM picture of CdSe thin film obtained at bath temperature of 80 °C; (b) SEM picture of CdSe:Fe thin film obtained at 0.01 M $FeSO_4$ concentration and at bath temperature of 80 °C.

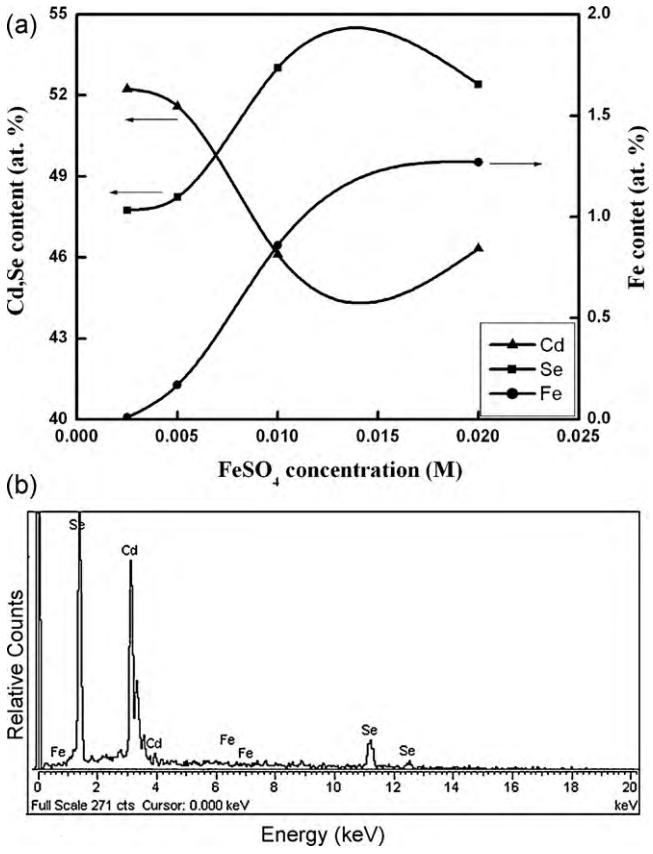

Fig. 7. (a) Typical EDX spectrum of CdSe:Fe thin film obtained at 0.01 M $FeSO_4$ concentration; (b) Variations of Cd, Fe and Se content with $FeSO_4$ concentration for CdSe:Fe thin films obtained at various $FeSO_4$ concentrations.

thin films which is evidenced from Fig. 6a and b. Increase in value of grain size favours coalescence between each grains during lateral growth which in turn explains increase in compactness of the deposited films. The sizes of the grains are found to be in the range between 0.41 and 0.83 μm. The average size of the grains is found to be 0.65 μm.

The film composition is analyzed using an energy dispersive analysis by X-rays. A representative EDX spectrum of CdSe:Fe thin films with Cd^{2+}, Fe^{2+} and H_2SeO_3 concentrations each of 0.01 M and 0.005 M TEA concentration is shown in Fig. 7a. The presence of emission lines Cd, Fe and Se in the investigated energy range shows the formation of CdSe:Fe thin films. Fig. 7b shows the variation of Cd, Se and Fe content with $FeSO_4$ concentration for CdSe:Fe thin films obtained at various $FeSO_4$ concentrations. It is observed from Fig. 7b that the content of Se increases and the content of Cd decreases while increasing the concentration of $FeSO_4$ from 0.0025 to 0.02 M. It is also observed that the content of Se increases while increasing $FeSO_4$ concentration from 0.0025 to 0.01 M, thereafter it decreases slightly. It is observed from Fig. 7b, upto 0.01 M $FeSO_4$ concentration, there is slight incorporation of Fe content in the film causes slight shift in XRD peaks. If the $FeSO_4$ concentration is increased above 0.01 M, the Fe content is increases above 1% which in turn causes decrease in value of FWHM data results decrease in value of crystallite size as shown in Fig. 5a [7,11]. Hence CdSe:Fe thin films with better crystallinity and stoichiometry is obtained at 0.01 M $FeSO_4$ concentration.

3.5. Optical properties

Optical transmittance of CdSe and CdSe:Fe films prepared at optimized $FeSO_4$ concentration of 0.01 M are recorded as a function of wavelength in the range between 300 and 1200 nm. Substrate absorption, if any is corrected by introducing an uncoated ITO substrate in the reference beam. The absorption coefficient (α) rises sharply owing to band-to-band transitions and levels off later. An analysis of absorption spectrum in the energy range 1.0 eV < hν < 3.5 eV represents that (α) follows the relation Eq. (7) [12].

$$\text{Absorptioncoefficient}\,(\alpha) = K/h\nu(h\nu - E_g)^{-1/2} \quad (7)$$

where α is the absorption coefficient in cm^{-1}, hν is the photon energy, K is a constant which is related to the effective masses associated with the valence and conduction band, E_g is gap between bottom of the conduction band and top of the valence band at the same value of wave vector. From the calculated values of absorption coefficient, a plot hν versus $(\alpha h\upsilon)^2$ is drawn for CdSe and CdSe:Fe films and shown in Fig. 8a,b. Extrapolation of linear portion of the graph to the energy axis (X-axis) is shown by curves a,b in Fig. 8 gives the band gap value of the material. The band gap values are found to be 1.73 eV for CdSe and 1.70 eV for CdSe:Fe thin films. It is observed that there is slight decrease in band gap observed for CdSe:Fe thin films. The decrease in value of band gap may be due to improvement of grain structure of the films which may be due to the segregation of impurity atoms along the grain boundaries [11,14,18]. The variation in refractive index and extinction coefficient with wavelength for CdSe and CdSe:Fe thin films are shown in Fig. 9a,b. Fig. 9.a,b reveals that both refractive index and extinction coefficient are decreases with respect to wavelength in the range between 350 and 1100 nm [19]. The band gap value of CdSe

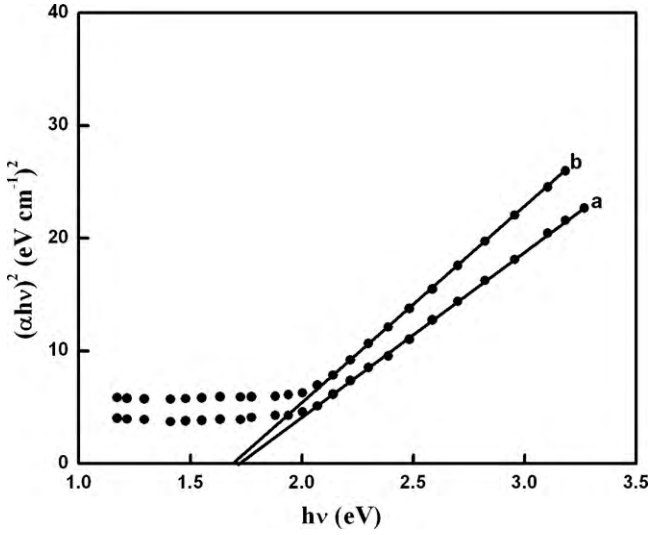

Fig. 8. Plot of hν versus $(\alpha h\nu)^2$: (a) CdSe (b) CdSe:Fe thin film obtained at 0.01 M $FeSO_4$ concentration.

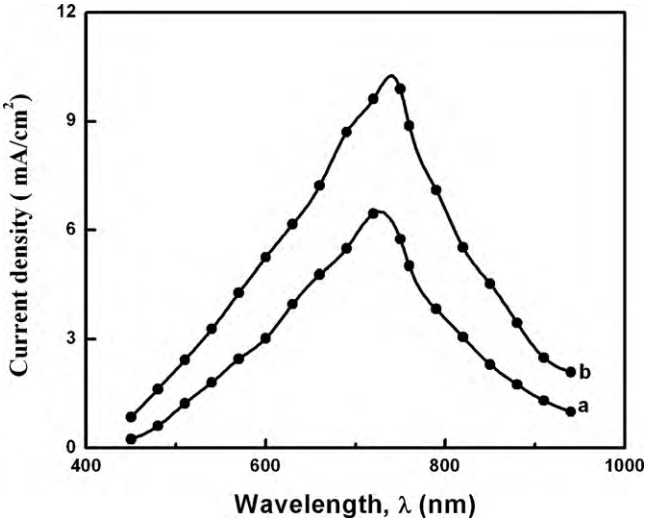

Fig. 10. Variation of photocurrent density with wavelength (λ) for:(a) CdSe (b) CdSe:Fe thin films.

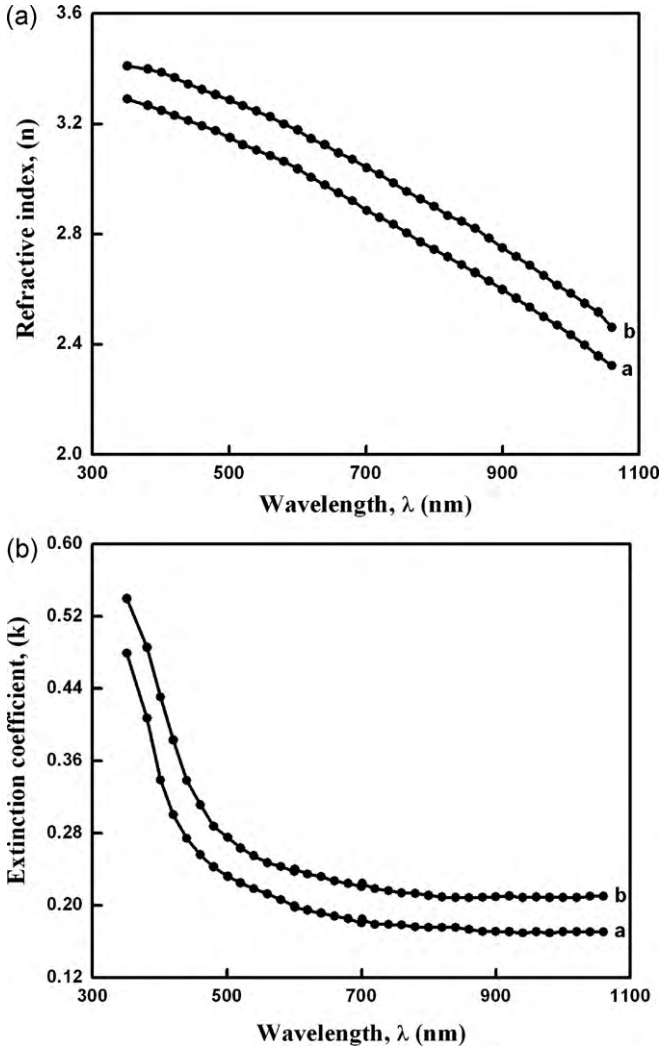

Fig. 9. (a) Variation of refractive index (n) with wavelength (λ):(a) CdSe (b) CdSe:Fe thin films obtained at 0.01 M $FeSO_4$ concentration; (b) Variation of extinction coefficient (k) with wavelength (λ): (a) CdSe thin film (b) CdSe:Fe thin films obtained at 0.01 M $FeSO_4$ concentration.

and CdSe:Fe thin films obtained in this work is found to be in close agreement with the value reported earlier [2,10].

3.6. Photoelectrochemical solar cell studies

From the point of view of photoelectrochemical solar cell (PEC) studies, n-type semiconducting materials endowed with acceptable stability and compatibility are required so that enhanced photoresponsivness to illumination may become possible. The quality of an electrodeposited semiconducting thin film needed for photovoltaic applications depends to a large extent on the applied deposition potential, the composition and pH of the electrolytic bath. PEC studies on CdSe and CdSe:Fe thin films are carried out in a conventional three electrode configuration with n-type CdSe and CdSe:Fe as photocathode, a platinum electrode and SCE as anode and reference electrode, respectively. The electrolyte consists of 1 M each of Na_2S, S and NaOH. A collimated light from tungsten filament (150W) lamp is used as the light source and spectral response measurements are carried out in the wavelength range between 550 and 950 nm using Keithley multimeter (Model 2000, USA). The variation in photocurrent density with respect to wavelength for CdSe and CdSe:Fe thin films are shown in Fig. 10. a,b. It is observed from Fig. 10 that the value of photocurrent density increases with wavelength and attained its maximum value at 720 and 740 nm for CdSe and CdSe:Fe thin films, thereafter the value of photocurrent density decreases with further increase of wavelength. The maximum value of photocurrent density corresponds well with the band gap for CdSe and CdSe:Fe thin films used in the present work for the preparation of photoelectrochemical device. The decrease in value of photocurrent density on shorter wavelength side may be due to the recombination of photogenerated carriers by surface states [20]. On the other hand the decrease in value of photocurrent density on longer wavelength side may be attributed to transition between defect levels [20]. Similar spectral response behaviour is reported earlier for Bi_2S_3 and Sb_2S_3 thin films [21,22]. Fig. 11 a,b shows the variation in open circuit voltage with short circuit current density for CdSe and CdSe:Fe thin films. PEC solar cell parameters such as open circuit voltage (V_{OC}), short circuit current density (I_{SC}), series resistance (R_S), shunt resistance (R_{Sh}), fill factor (FF), conversion efficiency (η) are evaluated from power output characteristics (Fig. 11 a,b). The above mentioned values are found to be 325 mV, 6.03 mA/cm^2, 44 Ω, 225 Ω, 0.36 and 0.88% for CdSe thin films. CdSe:Fe thin films have V_{OC}, I_{SC}, R_S, R_{Sh},

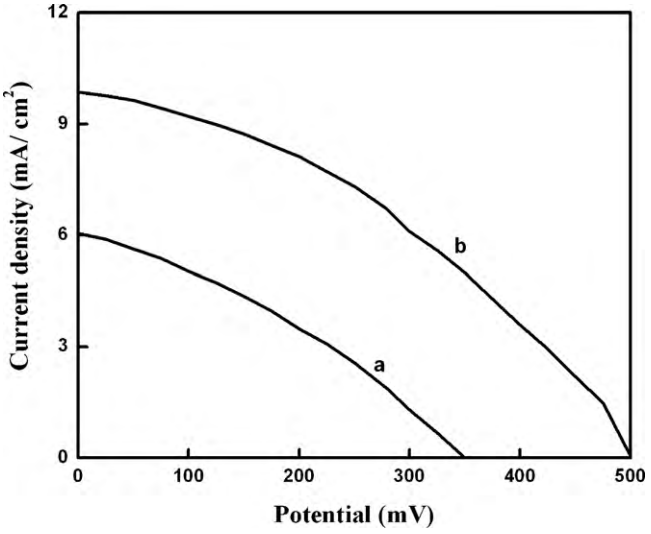

Fig. 11. Power output characteristics: (a) CdSe (b) CdSe:Fe thin films.

FF, η values 500 mV, 9.85 mA/cm^2, 39 Ω, 196 Ω, 0.38 and 2.21%, respectively.

4. Conclusions

Thin films of CdSe and CdSe:Fe are deposited on ITO substrates using potentiostatic electrodeposition technique. A cyclic voltammetric study is used to fix the deposition potential in the range between -1500 and +1500 mV versus SCE for CdSe and CdSe:Fe thin films. XRD patterns reveals that the deposited films exhibit hexagonal structure with preferential orientation along (002) plane. The microstructural parameters such as crystallite size, strain and dislocation density are calculated using XRD data and their dependency with $FeSO_4$ concentration are investigated. Morphological studies exhibits smooth surface with uniform spherical shaped grains for CdSe and CdSe:Fe thin films. Stoichiometric films of CdSe:Fe are obtained at 0.01 M $FeSO_4$ concentration. Optical properties of the deposited films indicates that decrease in value of refractive index and extinction coefficient are obtained for CdSe and CdSe:Fe thin films. Photoelectrochemical solar cell studies shows that the value of fill factor and efficiency are found to be 0.36, 0.88% for CdSe films and 0.38 and 2.21% for CdSe:Fe films.

Acknowledgement

One of the authors (S.Thanikaikarasan) gratefully acknowledge the Council of Scientific and Industrial Research (CSIR), New Delhi, India for the award of Senior Research Fellowship (SRF) with File No.:9/688(0010)2008 to carry out this work. The authors also thank FIST Programme, DST, New Delhi, India for providing X-ray diffraction facility to the Department of Physics, Alagappa University, Karaikudi, India.

References

[1] S.J. Lade, M.D. Uplane, C.D. Lokhande, Mater. Chem. Phys 68 (2001) 36–41.
[2] Cristian Baban, G.I. Rusu, Appl. Surf. Sci. 211 (2003) 6–12.
[3] R. Bhargava (Ed.), Properties of Wide bandgap Semiconductors, INSPEC Publications, London, 1997.
[4] Kehar Singh, Sameer S.D. Mishra, Solar Energ. Mater. Solar Cells 71 (2002) 115–129.
[5] Dong Hem, Kamal K. Mishra, Krishnan Rajeshwar, J. Electrochem. Soc 138 (1991) 100–108.
[6] U. Pal, D. Samanta, S. Ghorai, B.K. Samantaray, A.K. Chaudhuri, J. Phys. D: Appl. Phys 25 (1992) 1488–1494.
[7] G. Perna, V. Capaozzi, M. Ambrico, V. Augelli, T. Ligonzo, A. Minafra, L. Schiavulli, M. Pallara, Appl. Surf. Sci. 233 (2004) 366–372.
[8] R. Němec, D. MikeŠ, T. Rohovec, E. Uhlířovà, F. Trojànek, P. Malỳ, Mater. Sci. Eng. B 70 (2000) 500–504.
[9] V.S. John, T. Mahalingam, Jinn P. Chu, Solid State Electron. 49 (2005) 3–7.
[10] S.M. Pawar, A.V. Moholkar, K.Y. Rajpure, C.H. Bhosale, Appl. Surf. Sci. 253 (2007) 7313–7317.
[11] E.U. Masumdar, V.B. Gaikwad, V.B. Pujari, P.D. More, L.P. Deshmukh, Mater. Chem. Phys 77 (2002) 669–676.
[12] S. Thanikaikarasan, T. Mahalingam, K. Sundaram, A. Kathalingam, Taekyu Kim, Yong Deak Kim, Vacuum 83 (2009) 1066–1072.
[13] Cheng-min Shen, Xiao-gang Zhang, Hu-Lin Li, Mater. Sci. Eng. B 84 (2001) 265–270.
[14] G.S. Shahane, K.M. Garadkar, L.P. Deshmukh, Mater. Chem. Phys 51 (1997) 246–251.
[15] JCPDS-ICDD, File No.:08-0459,2003.
[16] S. Thanikaikarasan, T. Mahalingam, M. Raja, Taekyu Kim, Yong Deak Kim, J. Mater. Sci. Mater. Electron 20 (2009) 727–734.
[17] G.K. Williamson, R.E. Smallman, Philos. Mag 1 (1956) 34–46.
[18] U. Pal, S. Saha, A.K. Chaudhuri, V.V. Rao, H.D. Banerjee, J. Phys. D:Appl. Phys 22 (1989) 965–970.
[19] Suganthi Devadason, Muhamad Rasat Muhamad, Physica B 393 (2007) 125–132.
[20] Hosun Moon, A. Kathalingam, Thaiyan Mahalingam, J.P. Chu, Yong Deak Kim, J. Mater. Sci. Mater. Electron 18 (2007) 1013–1019.
[21] R.S. Mane, B.R. Sankapal, C.D. Lokhande, Mater. Chem. Phys 60 (1999) 158–162.
[22] R.S. Mane, C.D. Lokhande, Mater. Chem. Phys 78 (2002) 385–392.